VOLUME 35 NUMBER 4
APRIL 2017

ISSN: 1002-0721
CODEN JREAE 6

Journal of Rare Earths

ELSEVIER

Project for Enhancing International Impact of China STM Journals

CONTENTS

JOURNAL OF RARE EARTHS
Vol. 35 No. 4 (April 2017)

CONTENTS

SPECTROSCOPY, LUMINESCENCE AND PHOSPHORS

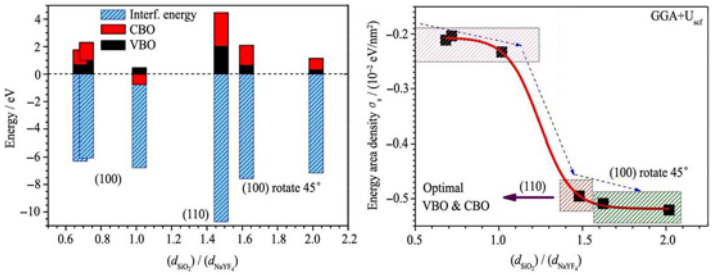

Left figure estimates thickness relative ratio dependent of valence band offsets (VBO) and conduction band offsets (CBO) for α-$NaYF_4$ and SiO_2 layers, with consideration of interface formation energy. Theab-initio DFT calculation shows the interface formation energy area density with related to the variation of shell-to-core thickness ratio (right figure). The results on different surface directions show well-fitted Boltzman function behavior for core-shell growth process

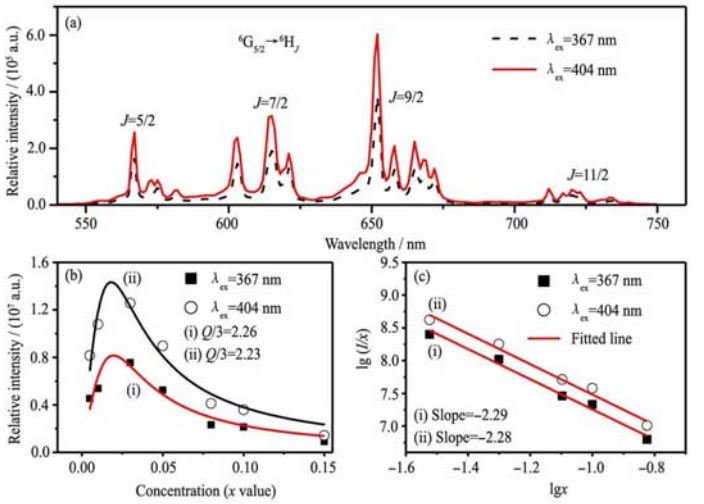

(a) Emission spectra of $Y_{2-x}Sm_xMoO_6$ (x=0.03) sample under 367 and 404 nm excitations; (b) The integrated emission intensity as a function of Sm^{3+} concentration; (c) Dependence of lg(I/x) versus lg(x) for $Y_{2-x}Sm_xMoO_6$ (x=0.03, 0.05, 0.08, 0.10, 0.15) samples

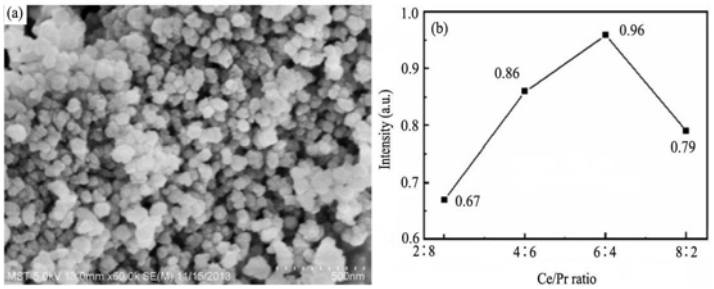

(a) SEM image of $(Ce_{0.6}Pr_{0.4})_{0.04}Y_{2.96}Al_5O_{12}$ nanoparticles, (b) PL emission intensity of $(Ce_xPr_{1-x})_yY_{0.04}Al_5O_{12}$ with different Ce/Pr ratio

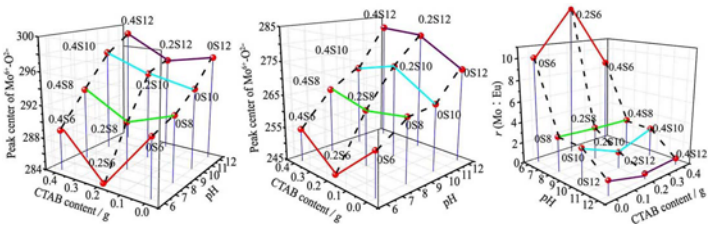

Center of CTB decomposition peaks and the relative intensity integral peak area ratio of Mo^{6+}-O^{2-} and Eu^{3+}-O^{2-} (r (Mo:Eu))

356 Luminescence properties of Eu^{3+} doped YBO_3 for temperature sensing

ZHAO Lu, CAO Zhongmin, WEI Xiantao, YIN Min, CHEN Yonghu

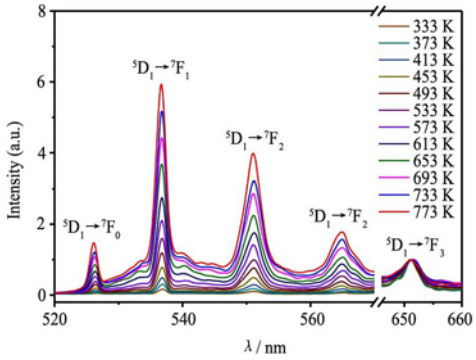

Temperature-dependent luminescence of $^5D_1 \rightarrow {}^7F_0$, $^5D_1 \rightarrow {}^7F_1$, $^5D_1 \rightarrow {}^7F_2$ and $^5D_0 \rightarrow {}^7F_3$

J. Rare Earths, (35) 2017: 356-360

361 Spectroscopic analysis of trivalent Nd^{3+}/Yb^{3+} ions codoped in PZS host glasses as a new laser material at 1.06 μm

B. Afef, H.H. Hegazy, H. Algarni, Y. Yang, K. Damak, E. Yousef, R. Maâlej

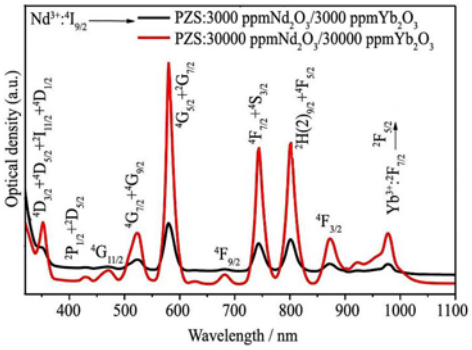

Absorption spectrum of phosphate glasses codoped with 3000 ppm and 30000 ppm Nd_2O_3/Yb_2O_3

J. Rare Earths, (35) 2017: 361-367

368 Crystal growth and spectral characterizations of Ho^{3+}-doped $Li_3Ba_2La_3(MoO_4)_8$ crystal

SONG Mingjun, ZHANG Nana, MENG Qingguo, WANG Lintong, LI Xiuzhi, WANG Guofu

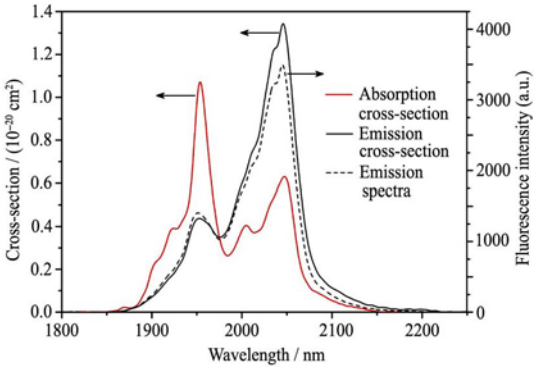

Unpolarized absorption and emission cross-sections for the $^5I_7 \rightarrow {}^5I_8$ transition of the Ho^{3+}: $Li_3Ba_2La_3(MoO_4)_8$

J. Rare Earths, (35) 2017: 368-373

RARE EARTH CATALYSIS

374 Sonication method synergism with rare earth based nanocatalyst: preparation of $NiFe_{2-x}Eu_xO_4$ nanostructures and its catalytic applications for the synthesis of benzimidazoles, benzoxazoles, and benzothiazoles under ultrasonic irradiation

Abolfazl Ziarati, Ali Sobhani-Nasab, Mehdi Rahimi-Nasrabadi, Mohammad Reza Ganjali, Alireza Badiei

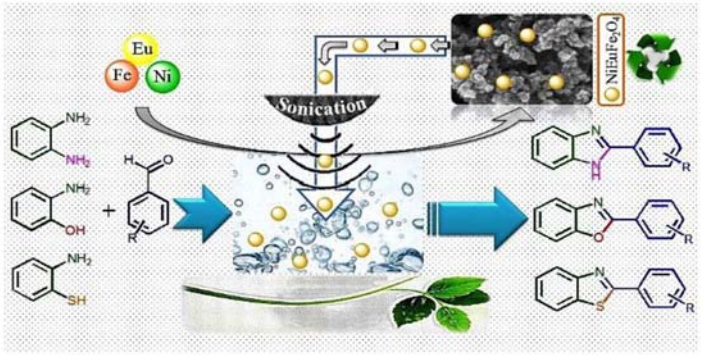

$NiFe_{2-x}Eu_xO_4$ as an efficient rare-earth based nanocatalyst for the synthesis of benzimidazoles, benzoxazoles, and benzothiazoles under ultrasonic irradiation

J. Rare Earths, (35) 2017: 374-381

ADVANCED RARE EARTH MATERIALS

382 Gd^{3+} doped $CuInS_2$/ZnS nanocrystals with high quantum yield for bimodal fluorescence/magnetic resonance imaging

YU Caiyan, XUAN Tongtong, LOU Sunqi, LIU Xiaoxiao, LIAN Guohai, LI Huili

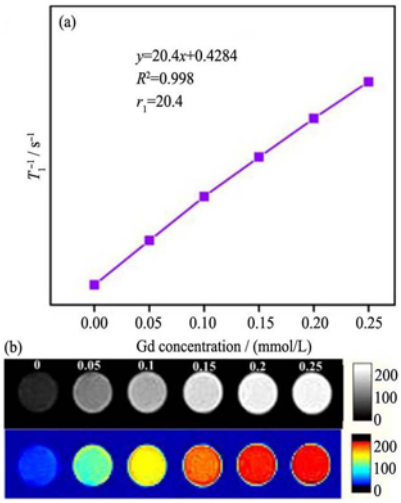

(a) Linear relationship between T_1^{-1} and Gd^{3+} concentrations, (b) T_1-weighted MRI (top) and corresponding pseudo-color images (bottom) of GCISZ NCs with different Gd^{3+} concentrations (The value of T_1^{-1} was collected basing on readings from (b))

J. Rare Earths, (35) 2017: 382-388

389 Synthesis and characterization of $Ce_{0.6}Sr_{0.4}Fe_{0.8}Co_{0.2}O_{3-\delta}$ perovskite material: Potential cathode material for low temperature SOFCs

Mlungisi N. Sithole, Bernard Omondi, Patrick G. Ndungu

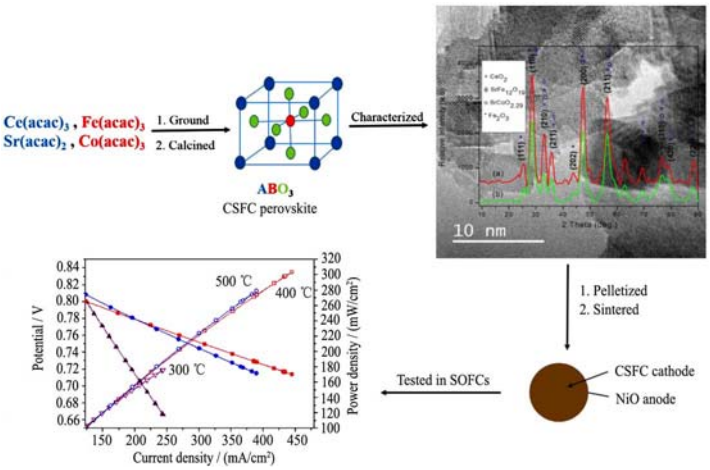

From synthesis to testing of ceria based perovskite materials for low temperature SOFCs

J. Rare Earths, (35) 2017: 389-397

CHEMISTRY AND HYDROMETALLURGY

398 Effects of mechanical activation on the kinetics of terbium leaching from waste phosphors using hydrochloric acid

TAN Quanyin, DENG Chao, LI Jinhui

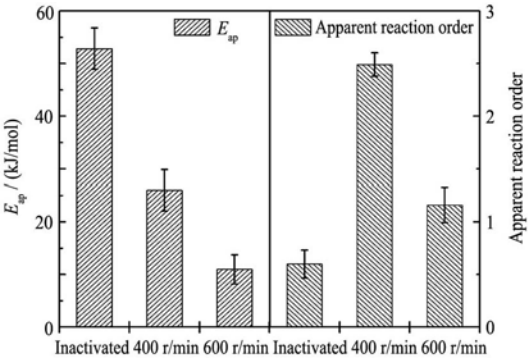

Effects of mechanical activation on apparent activation energy and reaction order of Tb leaching from inactivated and activated waste phosphors

J. Rare Earths, (35) 2017: 398-405

406 Evaluating corrosion resistances of Fe-based amorphous alloys by $Y^{Cr/Mo}$ values

XIA Huaixiao, CHEN Qingjun, WANG Chengjie

J. Rare Earths, (35) 2017: 406-411

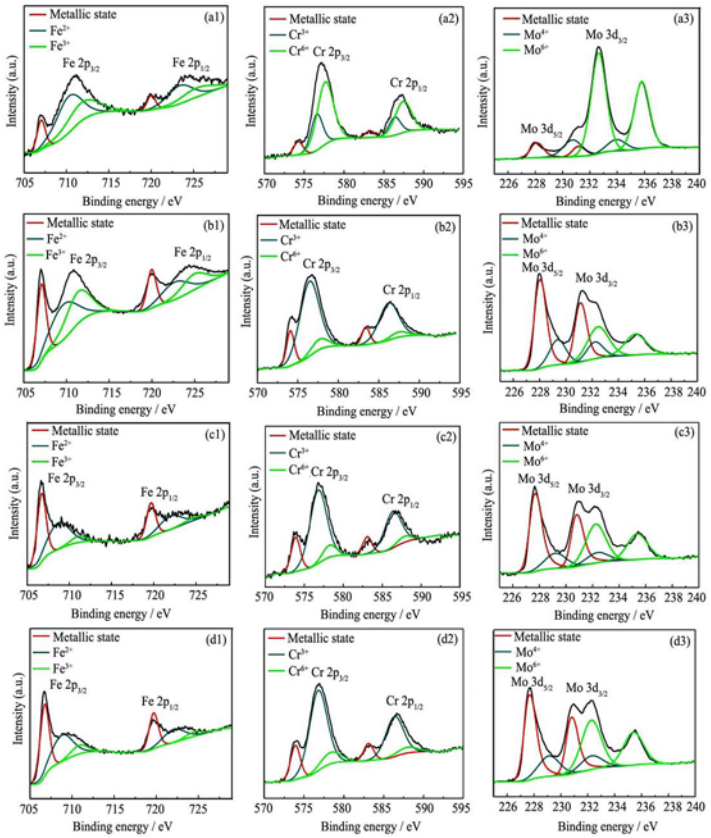

XPS spectra of Fe 2p, Cr 2p, and Mo 3d recorded from the surface of BMG2, BMG3 alloys after potentiostatic polarization at 0.25 and 0.5V_{SCE}; (a1–a3) BMG2 at 0.25 V, (b1–b3) BMG3 at 0.25V, (c1–c3) BMG2 at 0. 5V, (d1–d3) BMG3 at 0.5 V

METALLOGRAPHY AND PYROMETALLURGY

412 Microstructure and mechanical properties of Al-7Si-0.7Mg alloy formed with an addition of (Pr+Ce)

SONG Xianchen, YAN Hong, ZHANG Xiaojun

J. Rare Earths, (35) 2017: 412-418

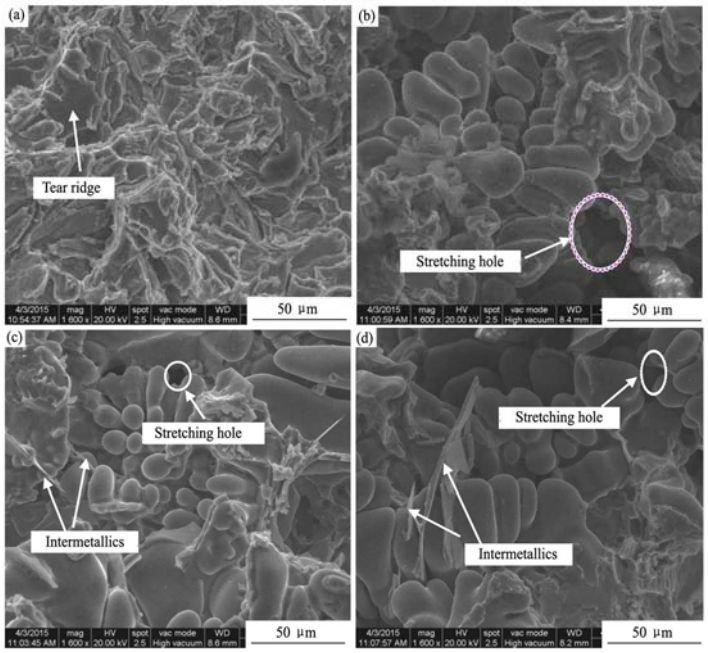

Fracture graphs of the tensile samples

(a) Unmodified; (b) 0.3% (Pr+Ce); (c) 0.6% (Pr+Ce); (d) 0.9% (Pr+Ce)